

## PERFORMANCE COMPARISON OF ED, TR AND DTR IR-UWB RECEIVERS FOR COMBINED PAM-PPM MODULATION IN REALISTIC UWB CHANNELS

H. A. Shaban\* and M. Abou El-Nasr

Arab Academy for Science, Technology & Maritime Transport (AASTMT), Abu Kir Campus, P. O. Box 1029, Alexandria, Egypt

**Abstract**—This paper studies the bit error rate (BER) performance of non-coherent impulse-radio ultra wideband (IR-UWB) correlation receivers in the IEEE 802.15.3a channel for combined binary pulse amplitude modulation-pulse position modulation (BPAM-PPM) scheme. The BER performance is based on the channel averaged signal-to-noise ratio (SNR). The study includes simple transmitted reference (TR), differential TR (DTR), and energy detection (ED) receiver structures. Moreover, different performance parameters are addressed, namely the signal bandwidth integration window factor, number of pulses per bit, and receiver power consumption. ED receivers with BPAM-PPM are shown to outperform simple TR receivers and have a performance which approaches that of differential TR (DTR) receivers with smaller power consumption for the same design parameters.

### 1. INTRODUCTION

Evolving applications of ultra wideband (UWB) technology, such as body area networks (BANs) and tele-healthcare are based on battery powered systems. In such systems, power consumption must be minimized. At the same time, these systems require the transmission of important data, which necessitates preserving a certain level of transmission accuracy. On the other hand, UWB channels are characterized by being dense multi-path channels. So, the receiver's performance robustness is an important factor in such challenging environments. Another important key design factor is the choice of the appropriate signaling technique. The two aforementioned key

---

*Received 9 December 2011, Accepted 22 February 2012, Scheduled 29 February 2012*

\* Corresponding author: Heba A. Shaban (hshaban@vt.edu).

factors, namely the choice of the receiver architecture together with the appropriate signaling technique are the two prominent factors in achieving low power consumption as well as performance robustness in dense multi-path channels [1–3].

Coherent receivers are the optimum solution for achieving robust performance in multi-path channels, however they require complex implementation as well as accurate channel estimation [4]. In particular, the template signal must be perfectly matched to the received signal, which is typically a delayed, attenuated, and distorted version of the transmitted signal [3,5,6]. On the other hand, non-coherent receivers do not require channel estimation, which is traded for bit error rate (BER) performance degradation as compared to optimum coherent detectors [7]. To date, non-coherent detectors are the most commonly used receivers in battery powered systems. Generally, non-coherent receiver architectures include simple transmitted reference (TR), differential TR (DTR), and energy detection (ED) receivers [8].

The main common modulation scheme employed with time hopping impulse-radio UWB (TH-IR-UWB) is the PPM modulation scheme, for which increasing the order of the pulse derivative leads to a smaller value of the minimal autocorrelation value and a consequently better BER performance. However, the achievement of a better BER performance is traded for higher sensitivity to timing jitter. Other common modulation techniques include, pulse amplitude modulation (PAM) and on-off keying (OOK) modulation [7]. The detection of OOK scheme requires the appropriate choice of the detection threshold, which needs to be constantly adapted to the variable channel conditions [6].

Combined PAM-PPM modulation scheme has been proposed in the literature as a good solution for optical line-codes [9]. Also, it has recently been proposed to be used with UWB communications [1,10,11]. This modulation scheme is characterized by achieving high data throughput [10]. Moreover, it does not have the high spectral lines associated with PPM signaling [11].

In this paper, we study and compare the performances of TR, DTR, and ED non-coherent IR-UWB detectors with binary PAM-PPM (BPAM-PPM) modulation scheme in the IEEE 802.15.3a channel [12]. The study includes some important factors that affect the performance of these detectors, such as the integration window bandwidth multiplication factor, number of pulses per bit, and power consumption. The evaluation of the BER is based on the channel-averaged signal-to-noise ratio (ASNR) using two approaches from the literature [13,14]. The organization of this paper is as follows.

Section 2 introduces the system model, and describes the studied receiver structures. The channel model and BER performance along with numerical results are given in Section 3. Conclusions are provided in Section 4.

## 2. SYSTEM MODEL AND STUDIED RECEIVER STRUCTURES

For an impulse-radio system based on time-topping (TH), the transmitted signal is given by:

$$s(t) = \sum_{i=0}^{N_s-1} \sqrt{E_s} b_{\lfloor i/N_s \rfloor} \omega(t - iT_f - c_i T_c - \delta d_{\lfloor i/N_s \rfloor}) \quad (1)$$

where,  $\omega(t)$  is the unit energy transmitted UWB pulse,  $E_s$  the energy per symbol,  $N_s$  the number of pulses per bit,  $b_{\lfloor i/N_s \rfloor}$  is the  $i$ -th data bit,  $\delta$  the time delay parameter for PPM,  $d_i$  the  $i$ -th data element position,  $c_i$  the  $i$ -th chip of the TH sequence,  $T_f$  the frame repetition time,  $T_c$  the chip duration, and  $\lfloor \cdot \rfloor$  the floor operator. For TR scheme, the transmitted signal is given by [10, 11]:

$$s_{TR}(t) = \sum_{i=0}^{\frac{N_s}{2}-1} \sqrt{E_s} \omega(t - iT_f - c_i T_c) + \sqrt{E_s} b_{\lfloor i/N_s \rfloor} \omega(t - iT_f - c_i T_c - \delta d_{\lfloor i/N_s \rfloor}) \quad (2)$$

For BPPM modulation,  $d_i = 1$ ,  $\delta \in \{0, T_c\}$ . Whereas, for BPAM modulation,  $d_i \in \{a_1, a_2\}$ ,  $\delta = 0$ . The corresponding parameters for combined BPAM-PPM modulation are  $d_i \in \{a_1, a_2\}$ ,  $\delta \in \{0, T_c\}$  [10, 11, 15]. According to [9], the BER performance of the optimum matched-filter detector in additive white Gaussian noise (AWGN) channel assuming BPAM modulation is given by  $P_e = 0.5 \operatorname{erfc}(\sqrt{\frac{(a_1 - a_2)^2}{8} SNR})$ , where,  $\operatorname{erfc}(\cdot)$  is the complementary error function and  $SNR$  is the signal-to-noise-ratio. The corresponding BER for BPAM-PPM modulation is given by  $P_e = \frac{1}{1.5} \operatorname{erfc}(\sqrt{\frac{(a_1 - a_2)^2}{8} SNR})$ .

This paper studies the BER performances of TR, DTR, and ED receivers in the IEEE 802.15.3a channel. In a nutshell, the TR scheme is based on the transmission of a pair of pulses (one modulated and one unmodulated), where at the receiver, the unmodulated pulse is used to detect the modulated pulse. However, TR correlation receivers suffer from the use of a noisy template [8]. Whereas, the differential transmitted reference (DTR) scheme uses the data pulses

of previous symbols for the correlation with the received pulses. Hence, DTR achieves a 3 dB performance gain over TR schemes. However, DTR requires differential encoding of the transmitted bits, which in turn requires longer delay lines, and consequently higher power consumption [8]. On the other hand, in the energy detection (ED), the correlator is replaced by a squaring device. The main difference between ED and TR receivers is the reference pulse. However, both receiver structures suffer from the use of noisy template waveforms, and both receivers require a careful choice of the integration window to minimize the BER performance [8,15]. The structure of the TR correlation receiver is shown in Figure 1(a), DTR receiver is shown in Figure 1(b), and ED correlation receiver is shown in Figure 1(c). Generally, ED receivers consume smaller amounts of power as compared to TR and fully digital architectures for the same design parameters. Figure 2 shows a comparison of the power consumption of four different receiver architectures based on the actual implementation parameters presented in [16,17]. As can be seen, ED receivers have the smallest power consumption as compared to TR and fully digital architectures. Moreover, for a 500 MHz signal bandwidth, ED receivers consume  $\approx$  half the power consumed by TR receivers for

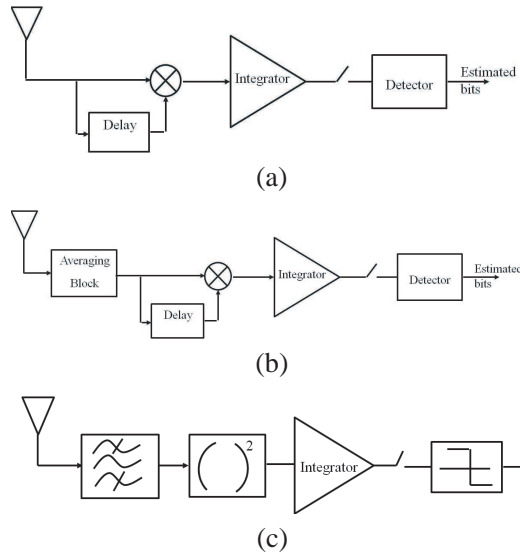


**Figure 1.** (a) Transmitted reference (TR) receiver structure [3]. (b) Differential TR (DTR) receiver structure [3]. And (c) Energy detection (ED) receiver structure [3].

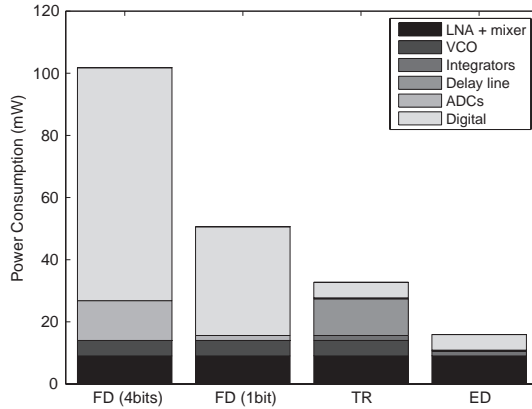


**Figure 2.** Power consumption comparison of 4-bit fully digital (FD), 1-bit FD, TR, and ED receiver architectures assuming a 500 MHz signal bandwidth.

the same design parameters. This difference in power consumption is intuitively because of the delay-element of the TR receiver, which consumes high power.

### 3. CHANNEL MODEL AND BER PERFORMANCE

In this section, we introduce the channel model and BER performance of the receivers under investigation based on the channel ASNR.

#### 3.1. Channel Model

The time-varying impulse response of a frequency selective fading channel can be written as [18]:

$$h(t, \tau) = \sum_k G_k(t) \delta(\tau - T_k(t)) \quad (3)$$

where,  $t$  and  $\tau$  are the observation and application times of the impulse response,  $k$  denotes the  $k$ -th multipath component,  $T_k(t)$  are the time-varying arrivals of the paths, and  $G_k(t)$  are the time-varying gains of the impulse [18]. For indoor channels, we consider the time-invariant model [18]:

$$h(\tau) = \sum_k G_k \delta(\tau - T_k) \quad (4)$$

The IEEE 802.15.3a channel model is a cluster-based model. Typically, the paths arrive in clusters with exponentially decaying amplitudes

that allow for multiple exponentially decaying sets [13]. The Poisson point process is used to model the multi-path arrival times  $T_k$ . The statistics of multi-path arrival times  $T_k$  and path gains  $G_k$  are specified by the IEEE 802.15.3a model [13, 18]. UWB channel measurements indicate that the amplitudes follow a lognormal distribution [18].

The IEEE 802.15.3a UWB channel model is treated as a two-dimensional point process of pairs  $(T_k, G_k)$  in [18] and [19] with the following channel response:

$$h(\tau) = \sum_k \phi(T_k, G_k) \quad (5)$$

where,  $\phi(T_k, G_k) = G_k \delta(\tau - T_k)$ , for which the channel response is represented as a sum of a function evaluated at random arguments, and is called a shot-noise random variable [18, 19]. If  $\phi(T_k, G_k)$  is set to be equal to  $G_k I_{[0, T_w]}(T_k)$ , where  $I_{[0, T_w]}(T_k)$  is an indicator function, then the sum represents the path gains that arrive in a time window  $[0, T_w]$ . This sum of gains is given by [18, 19]:

$$\Phi_l = \sum_k G_k I_{[0, T_w]}(T_k) \quad (6)$$

where, the indicator function of the  $l$ -th resolvable path within the interval  $[0, T_w]$  is  $I_{l[0, T_w]}(t) = 1$  for  $t \in [0, T_w]$  and is zero elsewhere, and  $T_w$  is chosen such that the expected energy in the finite interval  $[0, T_w]$  meets a specific fraction of the expected energy in the infinite observation window  $[0, \infty)$ , e.g., 90% of the expected energy [19].

In the context of multi-path channels, since the multi-path components are now defined as a two-dimensional point process of  $(T_k, G_k)$ , then the sum of path gains  $\Phi_l$  can be regarded as a counting measure of the paths that arrive within the measurable set of arrival times and path gains, where  $T_k \in [0, T_w]$  and  $G_k \in [G_{\min}, G_{\max}]$  [18].

The output signal-to-noise-ratio  $\Lambda$  is proportional to:

$$H_L = \sum_{l=0}^L \Phi_l^2 \quad (7)$$

where, random variable  $H_L$  is the sum of  $L + 1$  random variables with different distributions. The  $\Phi_l$  are uncorrelated but are not statistically independent. The corresponding average SNR as a function of number of paths  $L$  is [13]:

$$ASN R(L) = E[\Lambda] = SNR \times E[H_L] \quad (8)$$

where,

$$E[H_L] = \Omega_0 \{1 + R\bar{\beta}(T_w, s_0) + C\bar{\beta}(T_w, \tau_0) + RC[s_0\bar{\beta}(T_w, \tau_0) - s_0\bar{\beta}(T_w, s_0\tau_0/(s_0 - \tau_0))]e^{-T_w/s_0}\} \quad (9)$$

$T_w = (L + 1/2)T_\Delta$ ,  $T_\Delta = 1/W$ ,  $W$  is the signal bandwidth,

$$\bar{\beta}(T_w, \mu) = \int_0^{T_w} e^{-t/\mu} dt = \mu \left[ 1 - e^{-T_w/\mu} \right] \quad (10)$$

$E_b = N_s E_p$  is the bit energy,  $N_s$  the number of frames per bit,  $E_p$  the energy per pulse,  $R$  the ray arrival rate,  $C$  the cluster arrival rate,  $\tau_0$  the cluster decay factor,  $s_0$  is the ray decay factor, and  $\Omega_0$  a scale factor,  $\Omega_0 = 1/[(1 + Rs_0)(1 + C\tau_0)]$  [13]. Another definition for the channel averaged SNR is given in [14] in terms of the integration window  $T = L_p T_p$  ( $T$  is an  $L_p$  integer multiple of the pulse duration  $T_p$ ):

$$ASN R(L_p) = \frac{N_s E_p^2 G^2(L_p)}{N_0 E_p G(L_p) + N_0^2 B L_p T_p / 2} \quad (11)$$

where  $B$  is the one-sided receiver bandwidth, and the average path energy is calculated by enumerating all possible arrival times in the  $n$ -th time bin from  $G(L_p) \triangleq E\{A_i^{(1)2}\}$ ,  $E\{A_1^{(v)2}\} = \Omega_0$ , and

$$E\{A_n^{(v)2}\} = \Omega_0 P_c P_r \exp\left[-\frac{nT_\Delta}{s_0} + \frac{T_\Delta}{\tau_0}\right] \frac{\rho^2 (1 - \rho^{n-2})}{1 - \rho} + \Omega_0 P_c \exp\left[-\frac{(n-1)T_\Delta}{\tau_0}\right] + \Omega_0 P_r \exp\left[-\frac{(n-1)T_\Delta}{s_0}\right] \quad (12)$$

where,  $n \geq 2$ ,  $N$  is the number of time bins,  $P_c$  the probability that one cluster occurs with  $P_c = CT_\Delta$ , given the cluster arrival,  $P_r$  the probability that one ray occurs in a time bin with  $P_r = RT_\Delta$ ,  $\rho = \exp(\frac{T_\Delta}{s_0} - \frac{T_\Delta}{\tau_0})$ ,  $\bar{E}_c \triangleq E\{\sum_{i=1}^N A_n^{(v)2}\}$ , and  $\Omega_0 \triangleq \frac{1}{\bar{E}_c|_{\Omega_0=1}}$  [14].

### 3.2. BER Performance in the IEEE 802.15.3a Channel

In this subsection, we study the BER performance of TR, DTR, and ED receivers assuming the combined BPAM-PPM modulation scheme. The BER of simple TR receiver for BPAM is [7]:

$$P_b = E \left[ Q \left( \left[ \frac{2}{N_s} \left( \frac{N_0}{E_b} \right) + \frac{WT}{N_s} \left( \frac{N_0}{E_b} \right)^2 \right]^{-\frac{1}{2}} \right) \right] \quad (13)$$

where,  $E[\cdot]$  is the expected value,  $W$  the real bandpass signal bandwidth,  $Q(x) = \frac{1}{\sqrt{2\pi}} \int_x^\infty e^{-z^2/2} dz$ , and  $N_0$  the noise PSD. The BER

of TR receiver for BPAM-PPM is:

$$P_b = \frac{4}{3}E \left[ Q \left( \left[ \frac{2}{N_s} \left( \frac{N_0}{E_b} \right) + \frac{WT}{N_s} \left( \frac{N_0}{E_b} \right)^2 \right]^{-\frac{1}{2}} \right) \right] \quad (14)$$

The BER performance in Eq. (14) can be evaluated in two ways: (a) using Eq. (8) to evaluate Eq. (14) and (b) to use Eq. (11) to

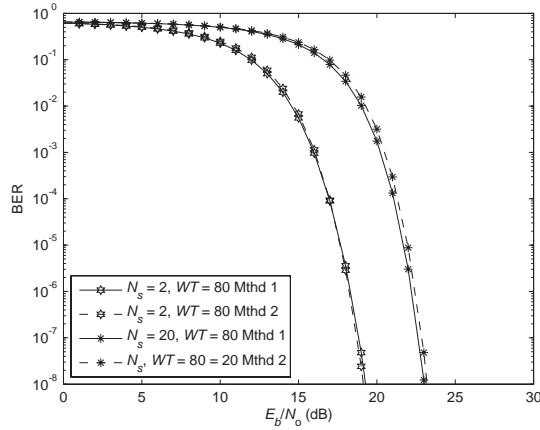


**Figure 3.** BER performance of TR-BPAM-PPM receiver in the IEEE 802.15.3a CM1 using two ways: (a) mthd. 1 [13] and (b) mthd. 2 [14] for  $N_s=2$  and 20.

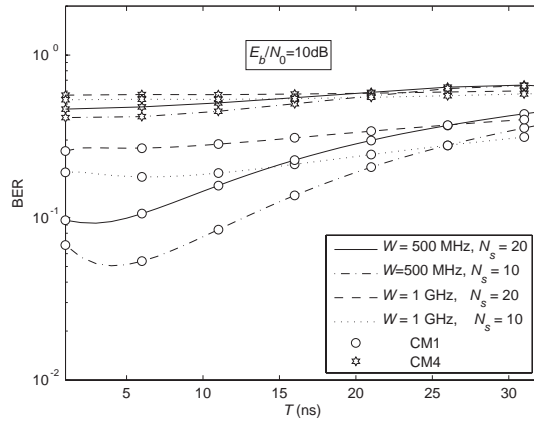


**Figure 4.** BER of TR-BPAM-PPM Rx. versus  $T$  (ns) for various  $W$  and  $N_s$  in CM1 and CM4.



evaluate Eq. (14). A comparison of the BER performance using the aforementioned two ways is shown in Figure 3 for  $N_s = 2$  and 20. As can be seen, the two methods give the same BER performance. Figure 4 depicts the BER performance of simple TR versus the integration window for BPAM-PPM modulation scheme in the IEEE 802.15.3a CM1 and CM4 channel models. As was previously mentioned, the integration window is an important factor that affects the performance of non-coherent detectors [8,15]. As can be seen in Figure 4, the optimum integration window is 6 ns for the TR receiver in the IEEE 802.15.3a CM1 and CM4 channel models.

The BER of DTR receiver for BPAM-PPM (DTR-BPAM-PPM) is:

$$P_b = \frac{4}{3}E \left[ Q \left( \left[ \frac{2N_s - 1}{N_s^2} \left( \frac{N_0}{E_p} \right) + \frac{WT}{4N_s} \left( \frac{N_0}{E_p} \right)^2 \right]^{-\frac{1}{2}} \right) \right] \quad (15)$$

The BER of ED receiver for BPPM (ED-BPPM) is [20]:

$$P_b = \frac{1}{2} \operatorname{erfc} \left( \frac{\eta(T) (d_0 + d_1 W) (E_b/N_0)}{2\sqrt{(TW/p_0) + 2s_0\eta(T) (E_b/N_0)}} \right) \quad (16)$$

where,  $\eta(T)$  is the ratio of the energy captured to the total energy available, and  $T$  denotes the integration window.  $d_0$ ,  $d_1$ , and  $s_0$  are

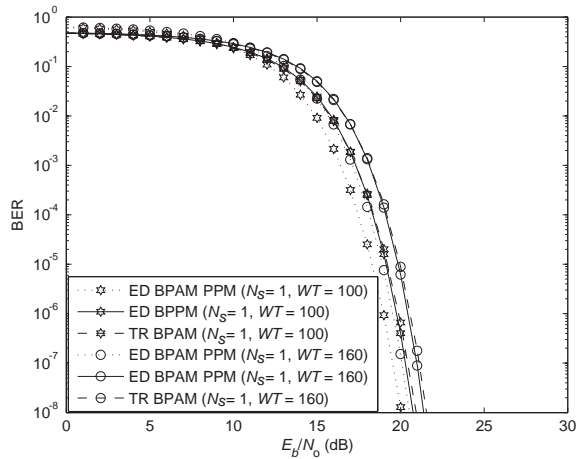


**Figure 5.** BER performance comparison of ED-BPPM, TR-BPAM, and ED BPAM-PPM receivers in the IEEE 802.15.3a CM4 for  $WT = 100$ , and 160.

IEEE 802.15.3a channel parameters [20]. The corresponding BER of ED receiver for BPAM-PPM (ED-BPAM-PPM) is:

$$P_b = \frac{1}{1.5} \operatorname{erfc} \left( \frac{\eta(T) (d_0 + d_1 W) (E_b/N_0)}{2\sqrt{(0.5TW/p_0) + 2s_0\eta(T) (E_b/N_0)}} \right) \quad (17)$$

Figure 5 shows a BER performance comparison between ED BPAM-PPM, ED-BPPM, and TR-BPAM. As can be seen, the ED-BPPM receiver achieves a similar BER performance to the TR-BPAM receiver [2]. Also, the ED-BPAM-PPM receiver outperforms TR-BPAM and ED-BPPM receivers. A BER performance comparison of DTR-BPAM-PPM and TR-BPAM-PPM correlation receivers in the IEEE 802.15.3a CM1 is shown in Figure 6. DTR outperforms TR receivers with 3 dB. Moreover, ED-BPAM-PPM receivers outperform TR-BPAM and ED-BPPM receivers as shown in Figure 5. This performance enhancement is traded for more sensitivity to timing mismatch of PPM schemes when compared to BPAM schemes. Figure 7 shows a performance comparison between ED-BPAM-PPM and DTR-BPAM-PPM receivers. As shown, both receivers have approaching performances. Nevertheless, ED-BPAM-PPM receiver require less power consumption as compared to ED-BPAM-PPM receiver.

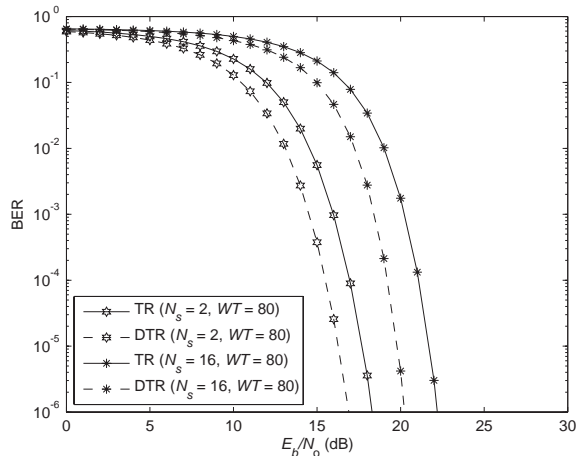


**Figure 6.** BER performance comparison of TR-BPAM-PPM and DTR-BPAM-PPM receivers in the IEEE 802.15.3a CM1 for  $N_s = 2$  and 16.

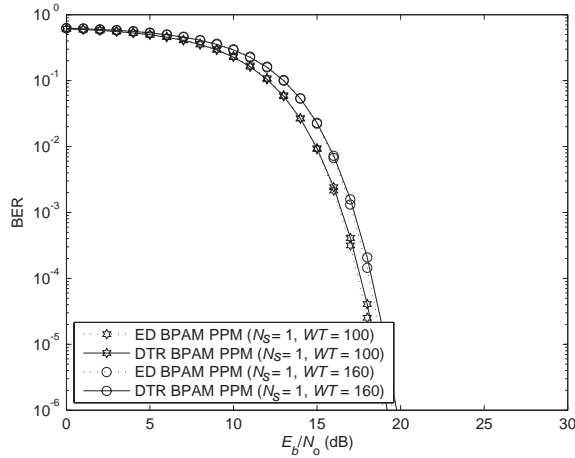


**Figure 7.** BER performance comparison of ED-BPAM-PPM and DTR-BPAM-PPM receivers in the IEEE 802.15.3a CM4 for  $WT = 100$  and 160.

#### 4. CONCLUSIONS

Non-coherent ED, TR and DTR correlation receivers were studied and compared in the IEEE 802.15.3a channel. In particular, we studied the performance of the aforementioned receivers with BPAM-PPM modulation, and compared their performances for BPPM and BPAM modulation schemes. Furthermore, the power consumption of the studied structures was compared based on actual implementation parameters. Ultimately, minimal BER and power consumption of studied receivers depend on signal bandwidth  $W$ , number of pulses per bit  $N_s$ , and integration window  $T$ . Moreover, it was shown that IR-UWB ED-BPPM-PAM receiver achieves a comparable BER to DTR-BPAM-PPM receiver with less power consumption, and outperforms TR receivers with BPAM-PPM modulation. Generally from the implementation point of view, ED receivers consume less power than TR receivers. The difference in power consumption is mainly caused by the analog delay line required for the correlation operation in the TR receivers. Typically, the performances of the studied receivers suffer from the use of noisy templates, and the achievement of a better BER performance requires the averaging of multiple received pulses. However, the ED-BPAM-PPM receiver outperforms the TR-BPAM and DTR-BPPM receivers.

## REFERENCES

1. Hirt, W. and M. Weisenhorn, "Robust non-coherent receiver for PAM-PPM signals," Patent 20 060 285 578, December 2006, [Online], Available: <http://www.freepatentsonline.com/y2006/0285578.html>.
2. Shaban, H., M. El-Nasr, and R. Buehrer, "A framework for the power consumption and BER performance of ultra-low power wireless wearable healthcare and human locomotion tracking systems via UWB radios," *2009 IEEE International Symposium on Signal Processing and Information Technology (ISSPIT)*, 322–327, 2009.
3. Shaban, H., "A novel highly accurate wireless wearable human locomotion tracking and gait analysis system via UWB radios," Ph.D. Dissertation, Virginia Tech., 2010.
4. Khani, H. and P. Azmi, "Performance analysis of a high data rate UWB-DTR system in dense multipath channels," *Progress In Electromagnetics Research B*, Vol. 5, 119–131, 2008.
5. Shaban, H., M. A. El-Nasr, and R. Buehrer, "Performance of ultralow-power IR-UWB correlator receivers for highly accurate wearable human locomotion tracking and gait analysis systems," *IEEE Global Telecommunications Conference, GLOBECOM 2009*, 1–6, Nov. 30–Dec. 4, 2009.
6. Reed, J. H. (ed.), *An Introduction to Ultra Wideband Communication Systems*, Prentice Hall, New Jersey, 2005.
7. Chao, Y.-L. and R. Scholtz, "Optimal and suboptimal receivers for ultra-wideband transmitted reference systems," *IEEE Global Telecommunications Conference, GLOBECOM 2003*, Vol. 2, 759–763 Vol. 2, Dec. 1–5, 2003.
8. Stoica, L., "Non-coherent energy detection trancivers for ultra wideband impulse radio systems," Ph.D. dissertation, University of Oulu Finland, 2008.
9. Bosotti, L. and G. Pirani, "A PAM-PPM signalling format in optical fibre digital communications," *Optical and Quantum Electronics*, Vol. 11, 71–86, 1979, 10.1007/BF00624059, [Online], Available: <http://dx.doi.org/10.1007/BF00624059>.
10. Abou-Rjeily, C., N. Daniele, and J.-C. Belfiore, "On high data rate space-time codes for ultra-wideband systems," *2005 IEEE International Conference on Ultra-Wideband, ICU 2005*, 1–6, 2005.
11. Shen, X., M. Guizani, R. C. Qiu, and T.-L. Ngoc (eds.), *Ultra-Wideband Communications and Networks*, 3rd edition, West John

- Wiley & Sons, Sussex, England, 2006.
12. Foerster, J., "Channel modeling sub-committee report final," *Doc: IEEE P802.15-02/490r1, Tech. Rep.*, Feb. 2003.
  13. Hao, K. and J. A. Gubner, "Performance measures and statistical quantities of rake receivers using maximal-ratio combining on the IEEE 802.15.3a UWB channel model," *IEEE Transactions on Wireless Communications*, 1–7, 2005.
  14. Jia, T. and D. I. Kim, "Analysis of channel-averaged SINR for indoor UWB rake and transmitted reference systems," *IEEE Transactions on Communications*, Vol. 55, No. 10, 2022–2032, Oct. 2007.
  15. Arslan, H., Z. N. Chen, and M.-G. D. Benedetto (eds.), *Ultra Wideband and Wireless Communication*, Wiley Interscience, New Jersey, 2006.
  16. Ryckaert, J., M. Verhelst, M. Badaroglu, S. Damico, V. De Heyn, C. Desset, P. Nuzzo, B. Van Poucke, P. Wambacq, A. Baschirotto, W. Dehaene, and G. Van der Plas, "A CMOS ultra-wideband receiver for low data-rate communication," *IEEE J. Solid-State Circuits*, Vol. 42, No. 1, 2515–2525, Nov. 2007.
  17. Verhelst, M. and W. Dehaene, "Analysis of the QAC IR-UWB receiver for low energy, low data-rate communication," *IEEE Transactions on Circuits and Systems I: Regular Papers*, Vol. 55, No. 8, 2423–2432, Sept. 2008.
  18. J. Gubner, "The IEEE 802.15.3a UWB channel model as a two-dimensional augmented cluster process," *IEEE Transactions on Information Theory*, Mar. 2006.
  19. Hao, K. and J. Gubner, "The distribution of sums of path gains in the IEEE 802.15.3a UWB channel model," *IEEE Transactions on Wireless Communications*, Vol. 6, No. 3, 811–816, Mar. 2007.
  20. Weisenhorn, M. and W. Hirt, "Robust noncoherent receiver exploiting UWB channel properties," *Joint International Workshop on Ultra Wideband Systems, 2004*, 156–160, May 18–21, 2004.